General Coupling Matrix Synthesis Methods for Chebyshev Filtering Functions

Richard J. Cameron, *Senior Member, IEEE*

***Abstract*— Methods are presented for the generation of the transfer polynomials, and then the direct synthesis of the corresponding canonical network coupling matrices for Chebyshev (i.e., prescribed-equiripple) filtering functions of the most general kind. A simple recursion technique is described for the generation of the polynomials for even- or odd-degree Chebyshev filtering functions with symmetrically or asymmetrically prescribed transmission zeros and/or group delay equalization zero pairs. The method for the synthesis of the coupling matrix for the corresponding single- or double-terminated network is then given. Finally, a novel direct technique, not involving optimization, for reconfiguring the matrix into a practical form suitable for realization with microwave resonator technology is introduced. These universal methods will be useful for the design of efficient high-performance microwave filters in a wide variety of technologies for application in space and terrestrial communication systems.**

***Index Terms*— Chebyshev characteristics, circuit synthesis methods, coupling matrix, microwave filters.**

I. Introduction

MICROWAVE filters incorporating the Chebyshev class of filtering function have, for many years, found frequent application within microwave space and terrestrial communication systems. The generic features of equiripple-amplitude in-band characteristics, together with the sharp cutoffs at the edge of the passband and high selectivity, give an acceptable compromise between lowest signal degradation and highest noise/interference rejection. The ability to build in prescribed transmission zeros for improving the close-to-band rejection slopes and/or linearizing the in-band group delay have enhanced its usefulness.

As the frequency spectrum becomes more crowded, specifications for channel filters have tended to become very much more severe. Very high close-to-band rejections are required to prevent interference to or from closely neighboring channels; at the same time, the incompatible requirements of in-band group-delay and amplitude flatness and symmetry are demanded to minimize signal degradation. All this is to be achieved with lowest insertion loss; on the high-power side to minimize the size, mass, and prime power consumption of RF power generation equipment and ease thermal management problems, and on the low-power (receive) side to reduce system noise figure if the filter is before or among the first amplification stages of the system.

Manuscript received February 18, 1998; revised January 13, 1999.

The author is with COM DEV Europe Ltd., Aylesbury, Bucks HP22 5SX, U.K.

Publisher Item Identifier S 0018-9480(99)02999-3.

In order to cope with the increasing demand for capacity in restricted spectral bandwidths, specifications for channel filter rejections have tended to become asymmetric. This is particularly true for the front-end transmit/receive (Tx/Rx) diplexers in the base stations of mobile communications systems, where very high rejection levels (sometimes as high as 120 dB) are needed from the Rx filter over the closely neighboring Tx channel's usable bandwidth and vice versa to prevent Tx-to-Rx interference. On the outer sides of the Tx and Rx channels, rejection requirements tend to be less severe. Such asymmetric rejection specifications are best met with asymmetric filtering characteristics, reducing filter degree to a minimum and, therefore, minimizing insertion loss, in-band distortions, and mass as compared with the symmetric equivalent achieving the same critical rejection levels.

In addition to the asymmetric feature, there is often a need for singly terminated designs. The singly terminated network has some special electrical properties which are useful for the design of manifold-coupled or star-coupled contiguous channel multiplexers and diplexers.

The methods to be presented in this paper are completely general for the design of the transfer functions and the synthesis of the prototype filter networks with characteristics belonging to the Chebyshev class of filtering function as follows:

1) even or odd degree;
2) prescribed transmission and/or group-delay equalization zeros;
3) asymmetric or symmetric characteristics;
4) singly or doubly terminated networks.

The first part of this paper describes an efficient recursive technique for generating the Chebyshev transfer and reflection polynomials, given the numbers and positions of the transmission zeros it is required to realize. This is followed by a summary of the method used to generate the corresponding coupling matrix. Having been well covered in previous papers [1]–[4], only the techniques used to deal with asymmetric characteristics will be detailed. Finally, a novel nonoptimization method is presented for directly reducing the coupling matrix resultant from the synthesis procedure, which, in general, will have all nonzero elements, to the more practical canonical folded network form. An example of usage is included.

A microwave filter may be realized directly from the folded coupling matrix, topology, and strengths of its inter-resonator couplings directly corresponding to the nonzero elements of the matrix. Recently, this has proven very useful for the design of dielectric resonator channel demultiplexer filters,

but more often, the folded network is used as the starting point for a further series of similarity transformations to convert the matrix into forms suitable for realizations in other technologies, e.g., [9] or [10].

II. Polynomial Synthesis

For any two-port lossless filter network composed of a series of N intercoupled resonators, the transfer and reflection functions may be expressed as a ratio of two Nth degree polynomials

$$S_{11}(\omega)=\frac{F_N(\omega)}{E_N(\omega)} \quad S_{21}(\omega)=\frac{P_N(\omega)}{\varepsilon E_N(\omega)} \tag{1}$$

where ω is the real frequency variable related to the more familiar complex frequency variable s by $s=j\omega$. For a Chebyshev filtering function, ε is a constant normalizing S_{21} to the equiripple level at $\omega=\pm 1$ as follows:

$$\varepsilon=\frac{1}{\sqrt{10^{RL/10}-1}}\cdot\left.\frac{P_N(\omega)}{F_N(\omega)}\right|_{\omega=1}$$

where RL is the prescribed return loss level in decibels and it is assumed that all the polynomials have been normalized such that their highest degree coefficients are unity. $S_{11}(\omega)$ and $S_{21}(\omega)$ share a common denominator $E_N(\omega)$, and the polynomial $P_N(\omega)$ contains the transfer function transmission zeros.

Using the conservation of energy formula for a lossless network $S_{11}^2+S_{21}^2=1$ and (1)

$$S_{21}^2(\omega)=\frac{1}{1+\varepsilon^2C_N^2(\omega)}=\frac{1}{(1+j\varepsilon C_N(\omega))(1-j\varepsilon C_N(\omega))} \tag{2}$$

where

$$C_N(\omega)=\frac{F_N(\omega)}{P_N(\omega)}.$$

$C_N(\omega)$ is known as the filtering function of degree N and has a form for the general Chebyshev characteristic [5]

$$C_N(\omega)=\cosh\left[\sum_{n=1}^{N}\cosh^{-1}(x_n)\right] \tag{3}$$

where

$$x_n=\frac{\omega-1/\omega_n}{1-\omega/\omega_n}$$

and $j\omega_n=s_n$ is the position of the nth transmission zero in the complex s-plane. It may be easily verified that when $|\omega|=1, C_N=1$, when $|\omega|<1, C_N\le 1$, and when $|\omega|>1, C_N>1$, all of which are necessary conditions for a Chebyshev response. Also, as all N of the prescribed transmission zeros approach infinity, C_N degenerates to the familiar pure Chebyshev function

$$C_N(\omega)_{|\omega_n\to\infty}=\cosh[N\cosh^{-1}(\omega)].$$

The rules to be observed when prescribing the positions of the transmission zeros are that symmetry must be preserved about the imaginary $(j\omega)$ axis of the complex s-plane to ensure that the numerator and denominator polynomials of $C_N(\omega)$ have purely real coefficients. Also, for the polynomial synthesis method about to be described, the number of transmission zeros with finite positions in the s-plane n_{fz} must be $\le N$. If $n_{fz}<N$, those zeros without finite positions must be placed at infinity. However, the two-port canonical networks to be used later to embody the transfer function will realize a maximum of $N-2$ finite-position zeros. When synthesizing the polynomials for these networks, at least two of the transmission zeros must be placed at infinity.

The aim now is to find the coefficients of the Nth degree polynomials in the variable ω corresponding to the right-hand side (RHS) of (3). With these polynomials, it is then possible to proceed to prototype network synthesis, from which a real electrical network with the transfer characteristic $S_{21}(\omega)$ of (1) may be derived.

The first step in the polynomial synthesis procedure is to replace the $\cosh^{-1}$ term in (3) with its identity

$$C_N(\omega)=\cosh\left[\sum_{n=1}^{N}\ln(a_n+b_n)\right] \tag{4}$$

where $a_n=x_n$ and $b_n=(x_n^2-1)^{1/2}$ Then,

$$\begin{aligned}C_N(\omega)&=\frac{1}{2}\left[\exp\left(\sum\ln(a_n+b_n)\right)+\exp\left(-\sum\ln(a_n+b_n)\right)\right]\\&=\frac{1}{2}\left[\prod_{n=1}^{N}(a_n+b_n)+\frac{1}{\prod_{n=1}^{N}(a_n+b_n)}\right].\end{aligned} \tag{5}$$

Multiplying the second term in (5)(top and bottom) by $\prod_{n=1}^{N}(a_n-b_n)$ yields

$$C_N(\omega)=\frac{1}{2}\left[\prod_{n=1}^{N}(a_n+b_n)+\prod_{n=1}^{N}(a_n-b_n)\right] \tag{6}$$

because $\prod_{n=1}^{N}(a_n+b_n)\prod_{n=1}^{N}(a_n-b_n)=\prod_{n=1}^{N}(a_n^2-b_n^2)$ in the bottom line of the second term will always be unity. This is easily verified by substituting for a_n and b_n using (4).

Equation (6) may now be written in its final form by substituting for a_n, b_n, and x_n using (3) and (4) as follows:

$$C_N(\omega)=\frac{1}{2}\left[\frac{\prod_{n=1}^{N}(c_n+d_n)+\prod_{n=1}^{N}(c_n-d_n)}{\prod_{n=1}^{N}\left(1-\frac{\omega}{\omega_n}\right)}\right] \tag{7}$$

where

$$\begin{aligned}c_n&=\omega-\frac{1}{\omega_n}\\d_n&=\omega'\left(1-\frac{1}{\omega_n^2}\right)^{1/2}\\\omega'&=(\omega^2-1)^{1/2}\end{aligned}$$

a transformed frequency variable.

By comparison with (2), it may be seen that the denominator of $C_N(\omega)$ is $P_N(\omega)$, the numerator polynomial of $S_{21}(\omega)$ generated from the prescribed transmission zeros ω_n. Also from (2), the numerator of $C_N(\omega)$ is the numerator $F_N(\omega)$ of $S_{11}(\omega)$, and appears at first to be a mixture of two finite-degree polynomials, one in the variable ω purely, while the other has each coefficient multiplied by the transformed variable ω'.

However, the coefficients multiplied by ω' will cancel with each other when (7) is multiplied out. This is probably best proven by demonstration, by multiplying out the left-hand side (LHS) and RHS product terms in the numerator of C_N in (7) for a few low values of n. In each case, it will be seen that the expansions will result in a sum of factors, each factor composed of multiples of c_n and d_n elements. Because of the positive sign in the LHS product term in (7), the c_n, d_n factors resultant from multiplying out the LHS term will always be positive in sign. Multiplying out the RHS product term in (7) will produce the same c_n, d_n factors; however, the negative sign will mean that those factors containing an odd number of d_n elements will be negative in sign and will cancel with the corresponding factors from the LHS product term.

The remaining factors will now contain only even numbers of d_n elements, and, therefore, $\omega'(=(\omega^2-1)^{1/2})$, which is a common multiplier for all the d_n elements [see (7)], will be raised by even powers only, thus producing subpolynomials in the variable ω only. Thus, the numerator of C_N will be a polynomial in the variable ω purely

These effects were used to develop a simple algorithm to determine the coefficients of the numerator polynomial of $C_N(\omega)$, $=F_N(\omega)$ the numerator of S_{11}.

A. Recursive Technique

The numerator of (7) may be rewritten as

$$\mathrm{Num}[C_N(\omega)] = F_N(\omega) = \frac{1}{2}\Big[G_N(\omega) + G'_N(\omega)\Big] \tag{8}$$

where

$$G_N(\omega) = \prod_{n=1}^{N}[c_n + d_n] = \prod_{n=1}^{N}\left[\left(\omega - \frac{1}{\omega_n}\right) + \omega'\left(1 - \frac{1}{\omega_n^2}\right)^{1/2}\right] \tag{9}$$

$$G'_N(\omega) = \prod_{n=1}^{N}[c_n - d_n] = \prod_{n=1}^{N}\left[\left(\omega - \frac{1}{\omega_n}\right) - \omega'\left(1 - \frac{1}{\omega_n^2}\right)^{1/2}\right]. \tag{10}$$

The method for computing the coefficients of $F_N(\omega)$ is basically a recursive technique where the solution for the nth degree is built up using the results of the $(n-1)$th degree. Considering first the polynomial $G_N(\omega)$ (9), this may be rearranged into two polynomials $U_N(\omega)$ and $V_N(\omega)$, where the $U_N(\omega)$ polynomial contains the coefficients of the terms in the variable ω only, while each coefficient of the auxiliary polynomial $V_N(\omega)$ is multiplied by the transformed variable ω' as follows:

$$G_N(\omega) = U_N(\omega) + V_N(\omega)$$

where

$$U_N(\omega) = u_0 + u_1\omega + u_2\omega^2 + \cdots + u_N\omega^N$$

and

$$V_N(\omega) = \omega'\big(v_0 + v_1\omega + v_2\omega^2 + \cdots + v_N\omega^N\big). \tag{11}$$

The recursion cycle is initiated with the terms corresponding to the first prescribed transmission zero ω_1, i.e., by putting $n = 1$ in (9) and (11) as follows:

$$\begin{aligned} G_1(\omega) &= [c_1 + d_1] \\ &= \left(\omega - \frac{1}{\omega_1}\right) + \omega'\left(1 - \frac{1}{\omega_1^2}\right)^{1/2} \\ &= U_1(\omega) + V_1(\omega). \end{aligned} \tag{12}$$

For the first cycle of the process, $G_1(\omega)$ has to be multiplied by the terms corresponding to the second prescribed zero ω_2 [see (9)] as follows:

$$\begin{aligned} G_2(\omega) &= G_1(\omega)\cdot[c_2 + d_2] \\ &= [U_1(\omega) + V_1(\omega)]\left[\left(\omega - \frac{1}{\omega_2}\right) + \omega'\left(1 - \frac{1}{\omega_2^2}\right)^{1/2}\right] \\ &= [U_2(\omega) + V_2(\omega)]. \end{aligned} \tag{13}$$

Multiplying out and again allocating terms purely in ω to $U_2(\omega)$, terms multiplied by ω' to $V_2(\omega)$, and recognizing that $\omega' V_n(\omega)$ will result in $(\omega^2-1)\cdot(v_0+v_1\omega+v_2\omega^2+\cdots+v_n\omega^n)$, a polynomial purely in ω and, therefore, to be allocated to $U_n(\omega)$ as follows:

$$\begin{aligned} U_2(\omega) &= \omega U_1(\omega) - \frac{U_1(\omega)}{\omega_2} + \left(1 - \frac{1}{\omega_2^2}\right)^{1/2}\omega' V_1(\omega) \\ V_2(\omega) &= \omega V_1(\omega) - \frac{V_1(\omega)}{\omega_2} + \left(1 - \frac{1}{\omega_2^2}\right)^{1/2}\omega' U_1(\omega). \end{aligned} \tag{14}$$

Having obtained these new polynomials $U_2(\omega)$ and $V_2(\omega)$, the cycle may be repeated with the third prescribed zero, and so on until all N of the prescribed zeros (including those at $\omega_n = \infty$) are used, i.e., $(N-1)$ cycles.

If the same process is repeated for $G'_N(\omega)$ $[=U'_N(\omega) + V'_N(\omega)$ as in (11)], then it will be found that $U'_N(\omega) = U_N(\omega)$ and $V'_N(\omega) = -V_N(\omega)$, and thus from (8) and (11) it may be seen that the numerator of $F_N(\omega)$ is equal to $U_N(\omega)$ after $(N-1)$ cycles of this recursion method. Now the reflection zeros may be found by rooting $G_N(\omega)$ and the denominator polynomial $E_N(\omega)$ found from (2) using, for example, the alternating singularity principle as described in [7].

To illustrate the procedure, the recursions will be applied to a fourth-degree example with an equiripple return-loss level of 22 dB and prescribed zeros at $+j1.3217$ and $+j1.8082$, chosen to give two attenuation lobe levels of 30 dB each on the upper side of the passband.

Initializing, using (12) with $\omega_1 = 1.3217$

$$\begin{aligned} U_1(\omega) &= -0.7566 + \omega \\ V_1(\omega) &= \omega'(0.6539). \end{aligned}$$

TABLE I
SINGULARITIES OF FOURTH-DEGREE ASYMMETRIC CHEBYSHEV FILTER WITH TWO PRESCRIBED TRANSMISSION ZEROS

	Reflection Zeros (Roots of $U_4(s)$ ($= F_4(s)$))	Transmission Zeros (Prescribed)	Transmission/ Reflection Poles (Roots of $E_4(s)$)	In-Band Reflection Maximae (Roots of $V_4(s)$)
1	$-j0.8593$	$+j1.3217$	$-0.7437 - j1.4178$	$-j0.4936$
2	$-j0.0365$	$+j1.8082$	$-1.1031 + j0.1267$	$+j0.3796$
3	$+j0.6845$	$j\infty$	$-0.4571 + j0.9526$	$+j0.8732$
4	$+j0.9705$	$j\infty$	$-0.0977 + j1.0976$	–

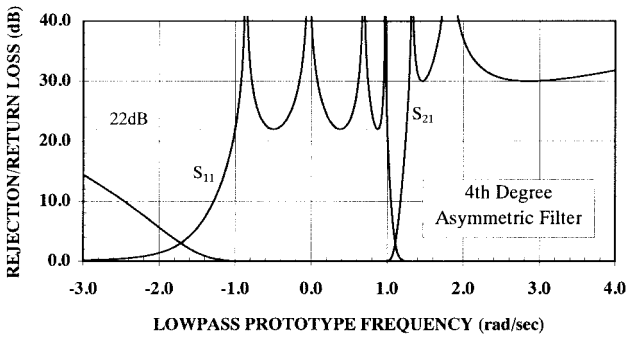

Fig. 1. Low-pass prototype transfer and reflection characteristics of fourth-degree asymmetric Chebyshev filter, with two prescribed transmission zeros at $+j1.3217$ and $+j1.8082$.

After the first cycle, with $\omega_2 = 1.8082$

$$U_2(\omega) = -0.1264 - 1.3096\omega + 1.5448\omega^2$$
$$V_2(\omega) = \omega'(-0.9920 + 1.4871\omega).$$

After the second cycle, with $\omega_3 = \infty$

$$U_3(\omega) = 0.9920 - 1.6134\omega - 2.3016\omega^2 + 3.0319\omega^3$$
$$V_3(\omega) = \omega'(-0.1264 - 2.3016\omega + 3.0319\omega^2).$$

After the third cycle, with $\omega_4 = \infty$

$$U_4(\omega) = 0.1264 + 3.2936\omega - 4.7717\omega^2 - 4.6032\omega^3 + 6.0637\omega^4$$
$$V_4(\omega) = \omega'(0.9920 - 1.7398\omega - 4.6032\omega^2 + 6.0637\omega^3).$$

At this stage, the polynomial $U_4(\omega)$ is the numerator of the reflection function $S_{11}(F_4(\omega))$, and rooting it will yield the N in-band reflection zeros. Rooting $V_4(\omega)$ will yield the $N-1$ in-band reflection maxima. The s-plane coordinates of these zeros, together with the corresponding transmission poles, are given in Table I, and plots of the transfer and reflection characteristics are given in Fig 1.

III. SYNTHESIS OF THE SINGLE- AND DOUBLE-TERMINATED COUPLING MATRIX

The procedure for synthesizing the coupling matrix from the transfer and reflection polynomials follows similar lines to those established in seminal papers by Atia *et al.* in the 1970's [1]–[4]. The methods are well-covered in these papers and will only be outlined below and in the Appendix, expanding where necessary to include the asymmetric case. The single-terminated case is included because of its usefulness for the design of contiguous-channel multiplexers where sometimes asymmetric characteristics are used, as well as symmetric. A topical example of such an application is in the Tx/Rx diplexers of cellular communications base stations, to obtain very high rejection levels over the contiguous Rx or Tx usable bands.

The starting point for the synthesis of the coupling matrix for both the single- and double-terminated cases are the transfer and reflection polynomials $E(s)$, $F(s)$, and $P(s)(s = j\omega)$, determined in the previous section as

$$S_{11}(s) = \frac{F(s)}{E(s)} \quad \text{and} \quad S_{21}(s) = \frac{P(s)}{\varepsilon E(s)}. \tag{15}$$

In the general case, the coefficients of $E(s)$ will be complex and those of $F(s)$ and $P(s)$ will alternate between purely real and purely imaginary as the power of s increases. The degree of $E(s)$ and $F(s)$ will be N, and the degree of $P(s)$ corresponds to the number of noninfinite zeros that were originally prescribed. As mentioned before, the successful synthesis of the two-port networks to be considered here depends on at least two of the transmission zeros being at infinity, therefore, the degree of $P(s)$ must not exceed $N-2$.

In this section, the synthesis of the rational polynomials for the short-circuit admittance parameters $y_{21}(=y_{12})$ and y_{22} from the transfer/reflection polynomials $E(s)$, $F(s)$, and $P(s)$ will be described. The procedure differs slightly for the single- and double-terminated cases and will be treated separately. The method used to synthesize the coupling matrix for the network from y_{21} and y_{22} will then be outlined.

A. Double-Terminated Case

Fig. 2(a) shows a two-port lossless filter network with a voltage source of internal impedance R_1 on the LHS and load impedance R_N to the RHS. The driving point impedance of this network in terms of its short- and open-circuit parameters is [11]

$$Z_{11}(s) = \frac{z_{11}[1/y_{22} + R_N]}{z_{22} + R_N} = \frac{z_{11}[1/y_{22} + 1]}{z_{22} + 1} \tag{16}$$

if R_N is normalized to 1 Ω [Fig 2(b)].

Also, if $R_1 = 1\ \Omega$, the driving point impedance

$$Z_{11}(s) = \frac{1 - S_{11}(s)}{1 + S_{11}(s)} = \frac{E(s) \pm F(s)}{E(s) \mp F(s)} = \frac{m_1 + n_1}{m_2 + n_2} \tag{17}$$

where m_1, m_2, n_1, and n_2 are complex-even and complex-odd polynomials, respectively, in the variable s constructed from $E(s)$ and $F(s)$.

For the even-ordered case, bringing n_1 outside the brackets of the numerator of (17) yields

$$Z_{11}(s) = \frac{n_1[m_1/n_1 + 1]}{m_2 + n_2}. \tag{18}$$

By comparing (18) and (16), it may be seen that

$$y_{22} = n_1/m_1 \tag{19}$$

and since the denominator of y_{21} is the same as that of y_{22}, and the numerator of y_{21} has the same transmission zeros as $S_{21}(s)$

$$y_{21} = P(s)/\varepsilon m_1. \tag{20}$$

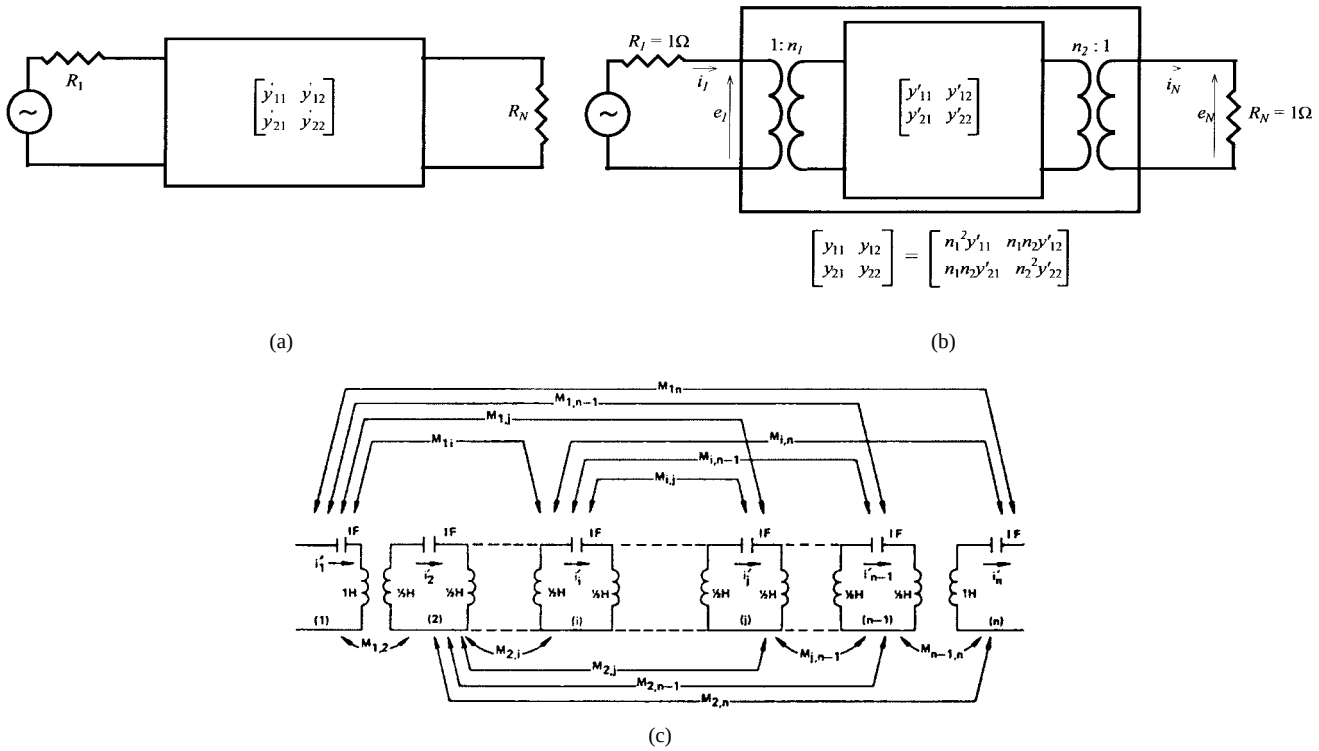

Fig. 2. General two-port cross-coupled network. (a) General two–port lossless network operating between source and load impedances R_1 and R_N. (b) Network with transformers to give unity terminating impedances. (c) "Inner" cross-coupled network.

Similarly,

$$y_{22} = m_1/n_1 \quad \text{and} \quad y_{21} = P(s)/\varepsilon n_1, \qquad \text{for } N \text{ odd.}$$

The complex-even and complex-odd polynomials m_1 and n_1 may be easily constructed from $E(s)$ and $F(s)$ by making use of (17) as follows:

$$m_1 + n_1 = \text{numerator of} Z_{11}(s) = E(s) + F(s).$$

Then,

$$m_1 = \text{Re}(e_o + f_o) + \text{Im}(e_1 + f_1)s + \text{Re}(e_2 + f_2)s^2 + \cdots$$

and

$$n_1 = \text{Im}(e_o + f_o) + \text{Re}(e_1 + f_1)s + \text{Im}(e_2 + f_2)s^2 + \cdots$$

where e_i and f_i, $i = 0, 1, 2, 3 \cdots N$ are the complex coefficients of $E(s)$ and $F(s)$. The above procedure ensures that both m_1 and n_1 will have purely real coefficients, and since the coefficients of the highest degree terms s^N in $E(s)$ and $F(s)$ are both purely real, and the degree of $P(s)$ is $<N$, that the common denominator of y_{22} and y_{21} is of degree N and the degree of each of their numerators is $<N$.

B. Single-Terminated Case

The construction of the polynomials m_1 and n_1 for the single-terminated case follows similar lines to the double-terminated procedure. For the single-terminated case, the source impedance $R_1 = 0$ and its transfer admittance $Y_{21}(s)$ may be expressed in terms of its short-circuit admittance parameters [3], [11]

$$Y_{21}(s) = \frac{y_{21}}{1 + y_{22}}, \qquad R_N = 1. \tag{21}$$

From (15)

$$\begin{aligned} S_{21}(s) &= \frac{P(s)/\varepsilon}{E(s)} \\ &= \frac{P(s)/\varepsilon}{m_1 + n_1} \\ &= \frac{P(s)/\varepsilon m_1}{1 + n_1/m_1}, \qquad \text{for } N \text{ even} \\ &= \frac{P(s)/\varepsilon n_1}{1 + m_1/n_1}, \qquad \text{for } N \text{ odd} \end{aligned}$$

where m_1 and n_1 are the complex-even and complex-odd polynomials constituting $E(s)$. For a single-terminated network with $R_N = 1$, the transfer function $S_{21}(s)$ equals the transfer admittance $Y_{21}(s)$ [11] and by comparing with (21) it may be seen that, for N even,

$$\begin{aligned} y_{21} &= P(s)/\varepsilon m_1 \\ y_{22} &= n_1/m_1 \end{aligned}$$

and for N odd

$$\begin{aligned} y_{21} &= P(s)/\varepsilon n_1 \\ y_{22} &= m_1/n_1 \end{aligned} \tag{22}$$

where

$$\begin{aligned} m_1 &= \text{Re}(e_0) + \text{Im}(e_1)s + \text{Re}(e_2)s^2 + \cdots \\ n_1 &= \text{Im}(e_0) + \text{Re}(e_1)s + \text{Im}(e_2)s^2 + \cdots \end{aligned}$$

and e_0, e_1, e_2, $\cdots$, etc., are the complex coefficients of $E(s)$ as before. Note that for the single-terminated case, it is only necessary to know ε, $P(s)$ and $E(s)$, the numerator and denominator of $S_{21}(s)$, to determine m_1 and n_1.

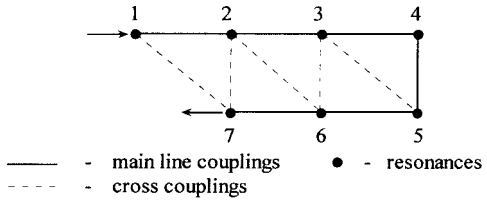

	1	2	3	4	5	6	7
1	s	m					xa
2	.	s	m			xa	xs
3	.	.	s	m	xa	xs	
4	.	.	.	s	m		
5	.	.	.	.	s	m	
6	.	.	.	.	.	s	m
7	.	.	.	.	.	.	s

Possible non-zero couplings:

s	–	self coupling
m	–	main line coupling
xa	–	asymmetric cross-coupling
xs	–	symmetric cross-coupling
.	–	couplings are symmetric about the principal diagonal

Fig. 3. Folded canonical network coupling matrix form—seventh-degree example. "s" and "xa" couplings are zero for symmetric characteristics.

C. Synthesis of the Coupling Matrix

Having determined the numerator and denominator polynomials of y_{21} and y_{22}, it is now possible to proceed to the synthesis of the coupling matrix of the electrical network. Under electrical analysis, this prototype network will precisely yield the same transfer and reflection characteristics as those embodied within the purely polynomial representations of $S_{11}(s)$ and $S_{21}(s)$.

The procedure for synthesizing the coupling matrix is almost unchanged from that originally established in [1], [2], and [4] for symmetric networks, and is outlined in the Appendix.

IV. Coupling-Matrix Reduction

The elements of the coupling matrix **M** that emerges from the synthesis procedure described in Section III will, in general, all have nonzero values. The nonzero values that will occur in the diagonal elements of the coupling matrices for electrically asymmetric networks represent the offsets from center frequency of each resonance (asynchronously tuned). Nonzero entries everywhere else means that in the network that **M** represents, couplings exist between every resonator node and every other resonator node. As this is clearly impractical, it is usual to annihilate couplings with a sequence of similarity transforms (sometimes called rotations) until a more convenient form with a minimal number of couplings is obtained. The use of similarity transforms ensures that the eigenvalues and eigenvectors of the matrix **M** are preserved, such that under analysis, the transformed matrix will yield exactly the same transfer and reflection characteristics as the original matrix.

There are several more practical canonical forms for the transformed coupling matrix **M**. Two of the better-known forms are the "right-column justified" (RCJ) form [8] and the more generally useful "folded" form [6] (Fig. 3). Either of these canonical forms may be used directly if it is convenient to realize the couplings or be used as a starting point for the application of further transforms to create an alternative resonator intercoupling topology, optimally adapted for the physical and electrical constraints of the technology with which the filter will eventually be realized, e.g., [9], [10]. The method for reduction of the coupling matrix to the folded form will be described here. The RCJ form may be derived using a very similar method.

	1	2	3	4	5	6	7
1	1						
2		1					
3			c_r		$-s_r$		
4				1			
5			s_r		c_r		
6						1	
7							1

$c_r \equiv \cos\theta_r$, $s_r \equiv \sin\theta_r$

Fig. 4. Example of seventh-degree rotation matrix $\mathbf{R}_r$-pivot [3, 5], angle θ_r.

A. Similarity Transformation and Annihilation of Matrix Elements

A similarity transform on an $N \times N$ coupling matrix $\mathbf{M}_0$ is carried out by pre- and post-multiplying $\mathbf{M}_0$ by an $N \times N$ rotation matrix $\mathbf{R}$ and its transpose $\mathbf{R}^t$ as follows:

$$\mathbf{M}_1 = \mathbf{R}_1 \cdot \mathbf{M}_0 \cdot \mathbf{R}_1^t$$

where $\mathbf{M}_0$ is the original matrix, $\mathbf{M}_1$ is the matrix after the transform operation, and the rotation matrix $\mathbf{R}$ is defined as in Fig. 4. The pivot $[i, j] (i \neq j)$ of $\mathbf{R}_r$ means that elements $R_{ii} = R_{jj} = \cos\theta_r$, $R_{ji} = -R_{ij} = \sin\theta_r$, $(i, j \neq 1 \text{ or } N)$, and θ_r is the angle of the rotation. All other entries apart from the principal diagonal are zero.

The eigenvalues of the matrix $\mathbf{M}_1$ after the transform are exactly the same as those of the original matrix $\mathbf{M}_0$, which means that an arbitrarily long series of transforms with arbitrarily defined pivots and angles may be applied, starting with $\mathbf{M}_0$. Each transform in the series takes the form

$$\mathbf{M}_r = \mathbf{R}_r \cdot \mathbf{M}_{r-1} \cdot \mathbf{R}_r^t, \qquad r = 1, 2, 3, \cdots, R \tag{23}$$

and under analysis the matrix $\mathbf{M}_R$ resultant at the end of the series of transforms will yield exactly the same performance as the original matrix $\mathbf{M}_0$.

When a similarity transform of pivot $[i, j]$ and angle $\theta_r (\neq 0)$ is applied to a coupling matrix $\mathbf{M}_{r-1}$, the elements in rows i and j and columns i and j of the resultant matrix $\mathbf{M}_r$ change in value from the corresponding element values in $\mathbf{M}_{r-1}$. For the kth element in the row or column i or j of $\mathbf{M}_r$, and not on the cross points of the pivot (i.e., $k \neq i, j$), the value will change according to the following formula:

$$\begin{aligned}
M'_{ik} &= c_r M_{ik} - s_r M_{jk}, && \text{for an element in row } i \\
M'_{jk} &= s_r M_{ik} + c_r M_{jk}, && \text{for an element in row } j \\
M'_{ki} &= c_r M_{ki} - s_r M_{kj}, && \text{for an element in column } i \\
M'_{kj} &= s_r M_{ki} + c_r M_{kj}, && \text{for an element in column } j
\end{aligned} \tag{24}$$

where $k (\neq i, j) = 1, 2, 3, \cdots, N$, $c_r = \cos\theta_r$, $s_r = \sin\theta_r$, and the undashed matrix elements belong to the matrix $\mathbf{M}_{r-1}$, and the dashed to $\mathbf{M}_r$.

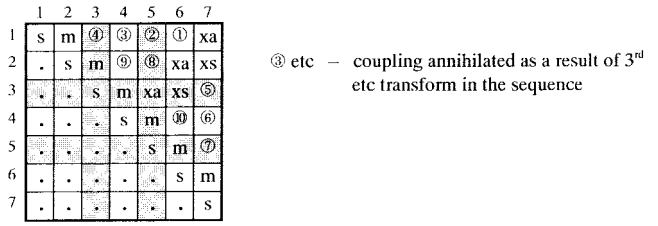

Fig. 5. Seventh-degree coupling matrix: reduction sequence for folded canonical form. The shaded elements are those that may be affected by a similarity transform at pivot [3, 5], angle θ_r. All others will be affected.

Two properties of a similarity transform which will be exploited for the matrix reduction process to be described below are noted here: 1) *only* those elements in the rows and columns i and j of the pivot $[i, j]$ of a transform may possibly be affected by the transform. All others will remain at their previous values and 2) if two elements facing each other across the rows and columns of the pivot of a transform are both zero before the application of the transform, they will still be zero after the transform. For example, if the elements M_{23} and M_{25} in Fig. 5 happen to be both zero before the transform with pivot [3, 5], they will still be zero after the transform, regardless of the transform angle θ_r.

The equations in (24) may be used to annihilate (zero) specific elements in the coupling matrix. For example, to annihilate a nonzero element M_{15} (and simultaneously M_{51}) in the coupling matrix of Fig. 5, a transform of pivot [3, 5] and angle $\theta_1 = -\tan^{-1}(M_{15}/M_{13})$ may be applied to the coupling matrix [see the last formula in (24) with $k = 1$, $i = 3$, $j = 5$]. In the transformed matrix, M'_{15} and M'_{51} will be zero and all values in rows and columns 3 and 5 (shaded in Fig. 5) may have changed.

The method for reducing the full coupling matrix $\mathbf{M}_0$ resultant from the synthesis procedure of Section III to the folded form of Fig. 3 involves applying a series of similarity transforms to $\mathbf{M}_0$ that annihilate unrealizable elements one by one. The transforms are applied in a certain order and pattern that makes use of the two effects mentioned above, ensuring that once annihilated, an element is not regenerated by a subsequent transform in the sequence.

B. Reduction Procedure—Full Coupling Matrix to Folded Canonical Form

There are a number of transform sequences that will reduce the full coupling matrix to the folded form. The sequence used here involves alternately annihilating elements right to left along rows and top to bottom down columns as shown in the seventh-degree example in Fig. 5, starting with the element in the first row and the $(N-1)$th column (M_{16}).

M_{16} may be annihilated with a transform of pivot [5, 6] and angle $\theta_1 = -\tan^{-1}(M_{16}/M_{15})$. This is followed by a second transform, pivot [4, 5], angle $\theta_2 = -\tan^{-1}(M_{15}/M_{14})$, which will annihilate element M_{15}. The previously annihilated element M_{16} is unaffected by this transform because it is lying outside the rows and columns of the latest pivot and remains at zero. Now, third and fourth transforms at pivots [3, 4] and [2, 3] and angles $\theta_3 = -\tan^{-1}(M_{14}/M_{13})$ and $\theta_4 = -\tan^{-1}(M_{13}/M_{12})$ will annihilate M_{14} and M_{13}, respectively, again without disturbing the previously annihilated elements.

TABLE II
SEVENTH-DEGREE EXAMPLE: SIMILARITY TRANSFORM SEQUENCE FOR REDUCTION TO THE FOLDED FORM. TOTAL NUMBER OF TRANSFORMS $R = \sum_{n=1}^{N-3} n = 10$ [SEE (23)]

Transform Number r	Element to be Annihilated		Pivot $[i, j]$	$\theta_r = \tan^{-1}(cM_{kl}/M_{mn})$				
				k	l	m	n	c
1	M_{16}	in 1st row	[5, 6]	1	6	1	5	–1
2	M_{15}	.	[4, 5]	1	5	1	4	–1
3	M_{14}	.	[3, 4]	1	4	1	3	–1
4	M_{13}	.	[2, 3]	1	3	1	2	–1
5	M_{37}	in 7th column	[3, 4]	3	7	4	7	+1
6	M_{47}	.	[4, 5]	4	7	5	7	+1
7	M_{57}	.	[5, 6]	5	7	6	7	+1
8	M_{25}	in 2nd row	[4, 5]	2	5	2	4	–1
9	M_{24}	.	[3, 4]	2	4	2	3	–1
10	M_{46}	in 6th column	[4, 5]	4	6	5	6	+1

After these four transforms, the elements in the first row of the matrix between the main line coupling M_{12} and the element in the final column will be zero. Due to the symmetry about the principal diagonal, the elements between M_{21} and M_{71} in the first column will also be zero.

Next, the three elements in column 7, M_{37}, M_{47}, and M_{57}, are annihilated with transforms at pivots [3, 4], [4, 5], and [5, 6] and angles $\tan^{-1}(M_{37}/M_{47})$, $\tan^{-1}(M_{47}/M_{57})$, and $\tan^{-1}(M_{57}/M_{67})$, respectively, [see first formula in (24)]. As with the rows, the columns are cleared down to the first main-line coupling encountered in that column. The couplings M_{13}, M_{14}, M_{15}, and M_{16} annihilated in the first sweep will remain at zero because they face each other across the pivot columns of the transforms of the second sweep and will, therefore, be unaffected.

Continuing on, a third sweep along row 2 annihilates M_{25} and M_{24} in that order, and the final sweep annihilates M_{46} in column 6. At this point, it may be seen that the form of the folded canonical coupling matrix has been achieved (Fig. 5), with its two cross diagonals containing the symmetric and asymmetric cross couplings. Table II summarizes the entire annihilation procedure.

The final values and positions of the elements in the cross diagonals are automatically determined—no specific action to annihilate couplings within them needs to be taken. As the number of finite-position prescribed transmission zeros that the transfer function is realizing grows from one to the maximum permitted ($N-2$), then the entries in the cross diagonals will progressively become nonzero starting with the asymmetric entry nearest to the principal diagonals (M_{35} in the seventh-degree example). If the original filtering function that the matrix is realizing is symmetric, then the asymmetric cross couplings M_{35}, M_{26}, and M_{17} will automatically be zero (as will the self couplings in the principal diagonal M_{11} to M_{77}).

The regular pattern and order of the annihilation procedure makes it very amenable to computer programming for any degree of coupling matrix.

TABLE III
SEVENTH-DEGREE ASYMMETRIC FILTER: COEFFICIENTS OF TRANSFER AND REFLECTION POLYNOMIALS. $\varepsilon = 6.0251$

s^n $n=$	Polynomial Coefficients		
	$P_N(s)$	$F_N(s)$	$E_N(s)$
0	$j1.0987$	$-j0.0081$	$0.1378-j0.1197$
1	-0.4847	0.0793	$0.8102-j0.5922$
2	$-j0.9483$	$-j0.1861$	$2.2507-j1.3346$
3	1.0	0.7435	$3.9742-j1.7853$
4		$-j0.5566$	$4.6752-j1.6517$
5		1.6401	$4.1387-j0.9326$
6		$-j0.3961$	$2.2354-j0.3961$
7		1.0	1.0

TABLE IV
COUPLING MATRIX BEFORE APPLICATION OF REDUCTION PROCESS. ELEMENT VALUES ARE SYMMETRIC ABOUT THE PRINCIPAL DIAGONAL. $R_1 = 0.7220$, $R_N = 2.2354$

	1	2	3	4	5	6	7
1	0.0586	-0.0147	-0.2374	-0.0578	0.4314	-0.4385	0
2	-0.0147	-0.0810	0.4825	0.3890	0.6585	0.0952	-1.3957
3	-0.2374	0.4825	0.2431	-0.0022	0.3243	-0.2075	0.1484
4	-0.0578	0.3890	-0.0022	-0.0584	-0.3047	0.4034	-0.0953
5	0.4314	0.6585	0.3243	-0.3047	0.0053	-0.5498	-0.1628
6	-0.4385	0.0952	-0.2075	0.4034	-0.5498	-0.5848	-0.1813
7	0	-1.3957	0.1484	-0.0953	-0.1628	-0.1813	0.0211

V. EXAMPLE OF USAGE

To illustrate the reduction procedure, an example is taken of a seventh-degree 23-dB return-loss single-terminated asymmetric filter, where a complex pair of transmission zeros at $\pm 0.9218 - j0.1546$ in the s-plane are positioned to give group-delay equalization over about 60% of the bandwidth, and a single zero is placed at $+j1.2576$ on the imaginary axis to give a rejection lobe level of 30 dB on the upper side of the passband.

With knowledge of the positions of the three Tx zeros, the numerator polynomial F_N of S_{11} may be constructed by the recursive technique of Section II, and then by using the given return loss and the constant ε, the denominator polynomial E_N common to S_{11} and S_{21} determined. The s-plane coefficients of these polynomials are given in Table III.

From these coefficients the numerators and denominators of y_{21} and y_{11} may be built up using (22). Being a single-terminated design, the coefficients of the polynomial F_N are not needed. Now, the residues resultant from the partial-fraction expansions of y_{21} and y_{11} will give the first and last rows of the orthogonal matrix $\mathbf{T}$ (A7). The remaining rows of $\mathbf{T}$ are found using an orthonormalization process and, finally, the coupling matrix $\mathbf{M}$ formed using (A4). The element values of $\mathbf{M}$ are given in Table IV.

To reduce this full coupling matrix to the folded form, a series of ten similarity transforms may now be applied to $\mathbf{M}$ according to Table II and (23). Each transform is applied to the coupling matrix resultant from the previous transform, starting with $\mathbf{M}$ [$= \mathbf{M_0}$ in (23)]. After the last of the transforms in the series, the nonzero couplings in the matrix $\mathbf{M}_{10}$ will topologically correspond with couplings between filter resonators arranged in a folded pattern, ready for direct realization in a suitable technology (Table V). Note that the couplings $\mathbf{M}_{17}$ and $\mathbf{M}_{27}$ in the cross diagonals, which are not needed to realize this particular transfer function, will automatically be zero. No specific action to annihilate them needs to be taken.

TABLE V
COUPLING MATRIX AFTER REDUCTION TO FOLDED FORM (M_{10})

	1	2	3	4	5	6	7
1	0.0586	0.6621	0	0	0	0	0
2	0.6221	0.0750	0.5977	0	0	0.1382	0
3	0	0.5977	0.0900	0.4890	0.2420	0.0866	0
4	0	0	0.4890	-0.6120	0.5038	0	0
5	0	0	0.2420	0.5038	-0.0518	0.7793	0
6	0	0.1382	0.0866	0	0.7793	0.0229	1.4278
7	0	0	0	0	0	1.4278	0.0211

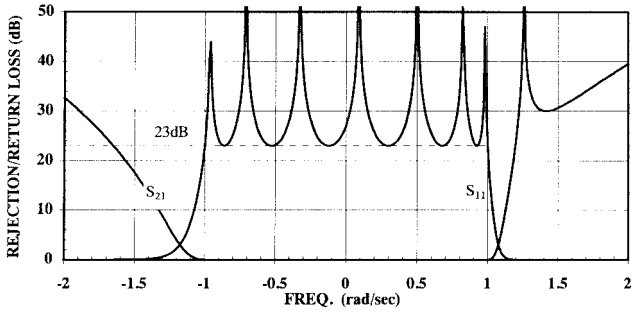

(a)

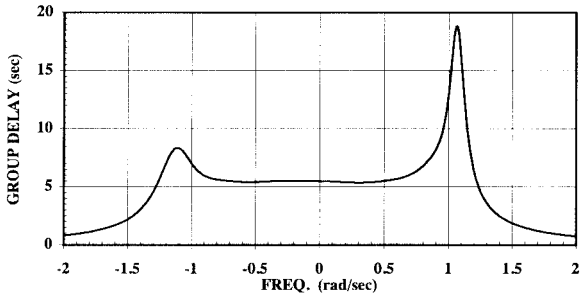

(b)

Fig. 6. Seventh-degree synthesis example: analysis of folded coupling matrix. (a) Rejection and return loss. (b) Group delay.

The results of analyzing this coupling matrix are given in Fig. 6(a) (rejection/return loss) and Fig. 6(b) (group delay). It may be seen that the 30-dB lobe level and equalized in-band group delay have not been affected by the transformation process.

Fig. 7(a) shows the topology of the folded network corresponding to the coupling matrix of Table V, and Fig. 7(b) shows a possible realization for the filter in coupled coaxial-resonator cavities. In this particular case, all the cross couplings happen to be the same sign as the main-line couplings, but in general, they will be mixed in sign.

VI. CONCLUSION

General methods have been presented for the generation of the transfer and reflection polynomials for the equiripple (Chebyshev) class of a filtering function with prescribed transmission zeros and then the efficient direct synthesis of the coupling matrix for the folded form of canonical network. If practical, microwave bandpass filters in a variety of technologies may be realized directly from the folded-network

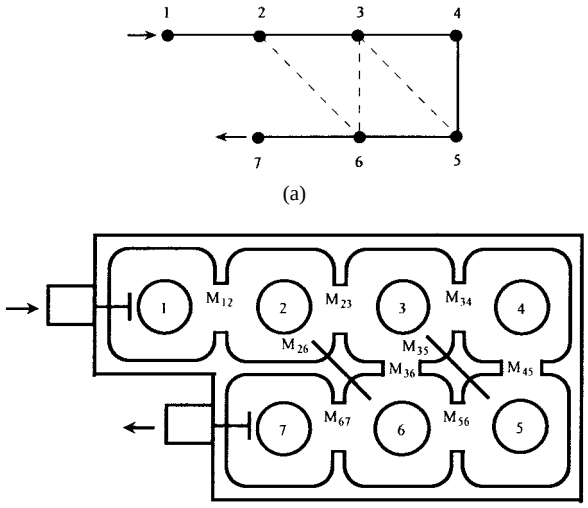

Fig. 7. Realization in folded configuration. (a) Folded network coupling and routing schematic. (b) Corresponding realization in coaxial-resonator technology.

coupling matrix or a further series of similarity transforms may be applied to reconfigure the coupling matrix to other more convenient forms. The methods are applicable for symmetric or asymmetric even- or odd-degree transfer characteristics; also for single- or double-terminated realizations.

No restrictions apply to the prescription of the finite-position transmission zeros to be built into the characteristics, except that the pattern of their positions must be symmetric about the imaginary axis of the complex s-plane, and their total numbers must not exceed $N-2$; N being the degree of the transfer characteristic.

APPENDIX

A. Synthesis of the Coupling Matrix

The source and load impedances R_1 and R_N of the general two-port network of Fig. 2(a) may be normalized to unity by the inclusion of transformers at the input and output of the network of turns ratio $1:n_1$ and $n_2:1$, respectively [Fig. 2(b)]. The "inner" general cross-coupled prototype bandpass network is shown in Fig. 2(c).

Since the prototype coupling coefficients and the network terminating impedances are assumed to be frequency invariant, the synthesis of the coupling matrix for this network may by done as a low-pass prototype after mapping with the formula $s = j[\omega_b - 1/\omega_b]$, where ω_b is the prototype bandpass frequency variable. For the prototype bandpass network, the center frequency and bandwidth are both 1 rad/s.

The two-port short-circuit admittance parameters relating to Fig. 2(b) are

$$\begin{bmatrix} i_1 \\ i_N \end{bmatrix} = \begin{bmatrix} y_{11} & y_{12} \\ y_{21} & y_{22} \end{bmatrix} \cdot \begin{bmatrix} e_1 \\ e_N \end{bmatrix}$$

of which $y_{21}\,(=y_{12})$ and y_{22} have both been determined already from the transfer/reflection functions as outlined in Section III. These parameters may be scaled through the transformers to represent the "inner" network in Fig. 2(c) giving

$$\begin{bmatrix} i_1 \\ i_N \end{bmatrix} = \begin{bmatrix} n_1^2 y'_{11} & n_1 n_2 y'_{12} \\ n_1 n_2 y'_{21} & n_2^2 y'_{22} \end{bmatrix} \cdot \begin{bmatrix} e_1 \\ e_N \end{bmatrix} \tag{A1}$$

where the dashed parameters relate to the inner network.

Referring now to the networks of Fig. 2(b) and (c), the loop equations may be represented in matrix form [4]

$$[j\,\mathbf{M} + s\,\mathbf{I} + \mathbf{R}] \cdot [i_1, i_2, i_3, \cdots, i_N]^t = e_1[1, 0, 0, \cdots, 0]^t \tag{A2}$$

where $\mathbf{R}$ is an $N \times N$ matrix with all entries zero, except $R_{11} = R_1$ and $R_{NN} = R_N$, $\mathbf{M}$ is the $N \times N$ reciprocal coupling matrix (i.e., $M_{ij} = M_{ji}$) and $\mathbf{I}$ is the identity matrix.

The short-circuit transfer admittance $y_{21}(s)$ of the overall network may be now determined by putting $s = j\omega$, R_1, and $R_N = 0$ (i.e., $\mathbf{R} = 0$), and solving (A2) for i_N as follows:

$$y_{21}(s) = \left.\frac{i_N}{e_1}\right|_{R_1,\, R_N=0} = j[-\mathbf{M} - \omega\,\mathbf{I}]^{-1}_{N1}$$

and similarly (by putting the voltage source at the other end of the network)

$$y_{22}(s) = \left.\frac{i_N}{e_N}\right|_{R_1,\, R_N=0} = j[-\mathbf{M} - \omega\,\mathbf{I}]^{-1}_{NN}. \tag{A3}$$

This is the essential step in the network synthesis procedure that relates the transfer function expressed in purely mathematical terms (i.e., S_{11}, y_{21}, etc., expressed as rational polynomials) to the real world of the coupling matrix, each element of which corresponds uniquely to a physical coupling element in the realized filter.

Since $\mathbf{M}$ is real and symmetric about its principal diagonal, all of its eigenvalues are real. Thus, an $N \times N$ matrix $\mathbf{T}$ with rows of orthogonal unit vectors exists, which satisfies the equation

$$-\mathbf{M} = \mathbf{T} \cdot \Lambda \cdot \mathbf{T}^t \tag{A4}$$

where $\Lambda = \mathrm{diag}[\lambda_1, \lambda_2, \lambda_3, \cdots, \lambda_N]$, λ_i are the eigenvalues of $-\mathbf{M}$ and $\mathbf{T}^t$ is the transpose of $\mathbf{T}$ such that $\mathbf{T} \cdot \mathbf{T}^t = \mathbf{I}$. Substituting (A4) into (A3) yields

$$\begin{aligned} y_{21}(s) &= j\left[\mathbf{T} \cdot \Lambda \cdot \mathbf{T}^t - \omega\,\mathbf{I}\right]^{-1}_{N1} \\ y_{22}(s) &= j\left[\mathbf{T} \cdot \Lambda \cdot \mathbf{T}^t - \omega\,\mathbf{I}\right]^{-1}_{NN}. \end{aligned} \tag{A5}$$

The general solution for an element i, j of an inverse eigenmatrix problem such as the RHS side of (A5) is

$$\left[\mathbf{T} \cdot \Lambda \cdot \mathbf{T}^t - \omega\,\mathbf{I}\right]^{-1}_{ij} = \sum_{k=1}^{N} \frac{T_{ik}\,T_{jk}}{\omega - \lambda_k}, \qquad i, j = 1, 2, 3, \cdots, N.$$

Therefore, from (A5),

$$y_{21}(s) = j \sum_{k=1}^{N} \frac{T_{Nk}\,T_{1k}}{\omega - \lambda_k}$$

and

$$y_{22}(s) = j \sum_{k=1}^{N} \frac{T_{Nk}^2}{\omega - \lambda_k}. \quad \text{(A6)}$$

Equations (A6) show that the eigenvalues λ_k of $-\mathbf{M}$ are also the roots of the denominator polynomial common to both $y_{21}(s)$ and $y_{22}(s)$ [this can also be seen from (A3)]. Thus, we can now develop the first and last rows T_{1k} and T_{Nk} of the orthogonal matrix $\mathbf{T}$ by equating the residues of $y_{21}(s)$ and $y_{22}(s)$ with $T_{1k}T_{Nk}$ and T_{Nk}^2, respectively, at corresponding eigenvalue poles λ_k. Knowing the numerator and denominator polynomials of $y_{21}(s)$ and $y_{22}(s)$ [(19), (20), (22)], their residues r_{21k} and r_{22k} may be determined from a partial fraction expansion, and then

$$T_{Nk} = \sqrt{r_{22k}}$$
$$T_{1k} = \frac{r_{21k}}{T_{Nk}} = \frac{r_{21k}}{\sqrt{r_{22k}}}, \qquad k = 1, 2, 3, \cdots, N. \quad \text{(A7)}$$

The transformer turns ratios n_1 and n_2 may be found by scaling the magnitudes of the row vectors T_{1k} and T_{Nk} to unity for the "inner" network of Fig. 2 as follows [see (A1)]:

$$n_1^2 = R_1 = \sum_{k=1}^{N} T_{1k}^2 \quad n_2^2 = R_N = \sum_{k=1}^{N} T_{Nk}^2.$$

Then,

$$T'_{1k} = T_{1k}/n_1$$

and

$$T'_{Nk} = T_{Nk}/n_2.$$

With the first and last rows of $\mathbf{T}'$ now determined, the remaining orthogonal rows may be constructed with the Gram–Schmidt orthonormalization process or equivalent and, finally, the coupling matrix $\mathbf{M}$ synthesized using (A4).

ACKNOWLEDGMENT

The author is grateful to Dr. A. Biswas, IIT Kanpur, India, for useful discussions, which clarified certain aspects of the theory and for proofreading the text of this paper, and to Dr. A. Atia, Orbital Sciences Corporation, Germantown, MD, for permission to use Fig 2(c).

REFERENCES

[1] A. E. Atia, A. E. Williams, and R. W. Newcomb, "Narrow-band multiple-coupled cavity synthesis," *IEEE Trans. Circuits Syst.*, vol. CAS-21, pp. 649–655, Sept. 1974.
[2] A. E. Atia and A. E. Williams, "Narrow-bandpass waveguide filters," *IEEE Trans. Microwave Theory Tech.*, vol. MTT-20, pp. 258–265, Apr. 1972.
[3] M. H. Chen, "Singly terminated pseudo-elliptic function filter," *COMSAT Tech. Rev.*, vol. 7, pp. 527–541, 1977.
[4] A. E. Atia and A. E. Williams, "New types of bandpass filters for satellite transponders," *COMSAT Tech. Rev.*, vol. 1, pp. 21–43, 1971.
[5] R. J. Cameron, "Fast generation of Chebychev filter prototypes with asymmetrically-prescribed transmission zeros," *ESA J.*, vol. 6, pp. 83–95, 1982.
[6] J. D. Rhodes, "A low-pass prototype network for microwave linear phase filters," *IEEE Trans. Microwave Theory Tech.*, vol. MTT-18, pp. 290–300, June 1970.
[7] J. D. Rhodes and A. S. Alseyab, "The generalized Chebychev low pass prototype filter," *Int. J. Circuit Theory Applicat.*, vol. 8, pp. 113–125, 1980.
[8] H. C. Bell, "Canonical asymmetric coupled-resonator filters," *IEEE Trans. Microwave Theory Tech.*, vol. MTT-30, pp. 1335–1340, Sept. 1982.
[9] R. J. Cameron and J. D. Rhodes, "Asymmetric realizations for dual-mode bandpass filters," *IEEE Trans. Microwave Theory Tech.*, vol. MTT-29, pp. 51–58, Jan. 1981.
[10] R. J. Cameron, "A novel realization for microwave bandpass filters," *ESA J.*, vol. 3, pp. 281–287, 1979.
[11] M. E. Van Valkenburg, *Introduction to Modern Network Synthesis.* New York: Wiley, 1960.

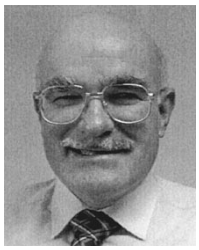

Richard J. Cameron (M'83–SM'94) was born in Glasgow, Scotland, in 1947. He received the B.Sc. degree in telecommunications and electronic engineering from Loughborough University, U.K., in 1969.

In 1969, he joined Marconi Space and Defense Systems, Stanmore, U.K. His activities there included small earth-station design, telecommunication satellite system analysis, and computer-aided RF circuit and component design. In 1975, he joined the European Space Agency's technical establishment (ESTEC, The Netherlands), where he was involved in the research and development of advanced microwave active and passive components and circuits, with applications to communications and earth observation spacecraft. Since joining COM DEV Ltd., Aylesbury, Bucks, U.K., in 1984, he has been involved in the development of software and methods for the design of high-performance components and subsystems for both space and terrestrial application.

Mr. Cameron is a member of the Institution of Electrical Engineers (IEE), U.K.